Article

Comparison of Huggins Coefficients and Osmotic Second Virial Coefficients of Buffered Solutions of Monoclonal Antibodies

Jai A. Pathak [1], **Sean Nugent** [1], **Michael F. Bender** [1], **Christopher J. Roberts** [2], **Robin J. Curtis** [3] and **Jack F. Douglas** [4,*]

[1] Vaccine Production Program (VPP), Vaccine Research Center (VRC), Formulation and Stabilization Sciences Department, National Institute of Allergy and Infectious Diseases (NIAID), National Institutes of Health (NIH), 9 W. Watkins Mill Rd., Gaithersburg, MD 20878, USA; jai.a.pathak@gmail.com (J.A.P.); sean.nugent@nih.gov (S.N.); michael.bender2@nih.gov (M.B.)

[2] Colburn Laboratory, Department of Chemical and Biomolecular Engineering, University of Delaware, Newark, DE 19716, USA; cjr@udel.edu

[3] Department of Chemical Engineering and Analytical Science, University of Manchester, Oxford Road, Manchester M13 9PL, UK; R.Curtis@manchester.ac.uk

[4] Materials Science and Engineering Laboratory, National Institute of Standards and Technology, 100 Bureau Drive, Gaithersburg, MD 20899-8544, USA

[*] Correspondence: jack.douglas@nist.gov

Abstract: The Huggins coefficient k_H is a well-known metric for quantifying the increase in solution viscosity arising from intermolecular interactions in relatively dilute macromolecular solutions, and there has been much interest in this solution property in connection with developing improved antibody therapeutics. While numerous k_H measurements have been reported for select monoclonal antibodies (mAbs) solutions, there has been limited study of k_H in terms of the fundamental molecular interactions that determine this property. In this paper, we compare measurements of the osmotic second virial coefficient B_{22}, a common metric of intermolecular and interparticle interaction strength, to measurements of k_H for model antibody solutions. This comparison is motivated by the seminal work of Russel for hard sphere particles having a short-range "sticky" interparticle interaction, and we also compare our data with known results for uncharged flexible polymers having variable excluded volume interactions because proteins are polypeptide chains. Our observations indicate that neither the adhesive hard sphere model, a common colloidal model of globular proteins, nor the familiar uncharged flexible polymer model, an excellent model of intrinsically disordered proteins, describes the dependence of k_H of these antibodies on B_{22}. Clearly, an improved understanding of protein and ion solvation by water as well as dipole–dipole and charge–dipole effects is required to understand the significance of k_H from the standpoint of fundamental protein–protein interactions. Despite shortcomings in our theoretical understanding of k_H for antibody solutions, this quantity provides a useful practical measure of the strength of interprotein interactions at elevated protein concentrations that is of direct significance for the development of antibody formulations that minimize the solution viscosity.

Keywords: monoclonal antibody; viscosity; Huggins coefficient; intrinsic viscosity; hard spheres; adhesive hard spheres; flexible polymers; second virial coefficient; static light scattering

1. Introduction

Recombinant proteins such as immunoglobulins (IgGs) are now routinely administered to patients at relatively high protein concentrations, often exceeding 100 mg/mL. Biopharmaceutical development scientists are confronted with serious challenges, primarily centered around protein aggregation [1–3], general colloidal instability, and elevated viscosity, η, all of which influence product stability and can render parenteral administration difficult [4,5]. Meanwhile, protein therapeutics provide relatively high in vivo potency, due to their large molecular weights and high required doses on the order of

1–2 mg/kg of the patient body weight and the relatively low dose volumes (<1.5 mL) required for subcutaneous drug administration [6]. At these high protein concentrations, the protein drug may "degrade" through aggregation and high solution viscosity, which are common challenges that must be overcome [1,7,8]. Specifically, the aggregation of a protein biotherapeutic can lead to reduced drug product potency and a greatly increased immunogenic response upon administration to patients [9–11]. The current pressing need for these highly concentrated protein therapeutics drives research in this field, especially antibody drugs. Then, the development of metrologies for quantifying protein–protein interactions, and for anticipating changes in the viscosity of protein solutions with changes in protein concentration and other changes in processing and clinical conditions, is a topic of intense scientific research and practical technological interest.

A discussion of the concentration dependence of viscosity can be mathematically framed in a virial framework, starting with the intrinsic viscosity, $[\eta]$. Intrinsic viscosity is defined in the zero-protein concentration (c_2) limit of the quotient of specific viscosity, η_{SP}, and c_2. Tanford demonstrated that $[\eta]$ is an appropriate dilute solution viscometric descriptor [12], as in the case of synthetic polymer solutions [13],

$$[\eta] = \underset{c_2 \to 0}{Lim} \frac{\eta_{SP}}{c_2} = \underset{c_2 \to 0}{Lim} \frac{\eta - \eta_S}{\eta_S c_2} \tag{1}$$

Below, η_S and η denote buffer and protein solution viscosity, respectively. The relative viscosity of the protein solution, η_R, can be defined as $\eta_R = \eta/\eta_S$ and is directly related to the specific viscosity ($\eta_{SP} = \eta_R - 1$). The relative viscosity can also be expressed as a virial expansion power series in the solute (protein) concentration:

$$\eta_R = 1 + [\eta]\, c_2 + k_H \left([\eta]\, c_2\right)^2 + \dots. \tag{2}$$

The second hydrodynamic virial coefficient or "Huggins coefficient" k_H is defined in the concentration regime where two-body interactions dominate, similar to the osmotic second virial coefficient, B_{22}, which is obtained from osmotic pressure measurements. By providing a hydrodynamic measurement of inter-protein interactions, specifically the effect on the solution viscosity for IgG solutions beyond the dilute regime, k_H may shed new insights into our understanding of crowded protein solution physics. The studies presented here explore the hypothesis that the hydrodynamic information provided by k_H, as well as contributions to thermodynamic and conformational information, may be of significant value in characterizing protein solutions at elevated protein concentrations.

An in-depth examination of k_H also offers an opportunity to scrutinize and evolve classical theories regarding the intrinsic physical nature of proteins. Recent work by the authors [14–16] has explored the hypothesis that proteins are better idealized as polymeric structures rather than colloidal hard spheres, which is a subject of great relevance to modeling the solution hydrodynamic and thermodynamic properties of these macromolecules. Negatively and positively charged patches are present on protein molecules, suggesting that these systems might be idealized as patchy colloidal particles [17] (We discuss the rationale of this simple protein model below). The colloidal depiction has often been assumed to be a reasonable initial model for relatively compact proteins in their native globular state where deviations from the spherical shape are relatively small compared to swollen linear polymers [18]. However, the invocation of a colloidal model of proteins should not preclude a consideration of models that incorporate a description of directional interactions and molecular structure and variations in the rigidity of these molecules, and we discuss some of these models below. The solution properties of monoclonal antibodies examined in this paper are compared to the classic hard sphere colloid and flexible polymer models as zero-order reference models with a view toward developing an adequate minimal model of these protein solutions.

Inter-protein interactions in the solution state can be generally divided into short-range "SR" attractive/adhesive interactions (hydrophobic, van der Waals, H-bonding,

excluded volume, etc.) and long-range "LR" interactions, which are typically electrostatic in nature (monopole, dipole, quadrupole, etc.) (We discuss these interactions and their significance for the properties of antibody solutions in a separate section below.). Solution ionic strength (*I*) is a convenient experimental tool to turn LR electrostatics "on" at low *I* or "off" at high *I* by adding salt to screen electrostatic interactions through the Debye screening effect. The application of this model seems to be most suitable for the high *I* regime, where the electrostatic screening should be especially great, as postulated by Kastelic et al. [19]. With these assumptions in mind, we consider the adhesive or "sticky" sphere model of Russel [20], henceforth referred to as the "Russel model", as a potentially suitable coarse-grained of protein/antibody solutions with appreciable salt and concentrations below the infinite dilute limit as well as below the concentrated solution regime. We emphasize that Russel's simplified hydrodynamic model for k_H neglects charge, dipole interactions, and protein conformation effects that are clearly important in protein solutions so that the applicability of this model, even in the high salt, remains a question that must currently be decided by measurement in the absence of any theory of sufficient generality to describe all the potential interactions that one might consider as being possibly relevant to the complex solutions. The Russel model is a "coarse-grained" model, which is a dignified way of saying that it involves radical approximations. Despite the limitations apparent in this type of model, it still provides a benchmark model against we may gauge the behavior of real protein solutions, and we may hope that the dimensionless reduced variables defined by this model might have a greater validity than the model itself, as in the case of van der Waals model of the equation of state of liquids.

Russel's simple model of k_H of particles having attractive interparticle interactions extends the classical calculation of Batchelor [21] to account for Brownian stress contributions to hard sphere interparticle interactions modeled by the classical Baxter sticky hard sphere model [22]. In this context, the "strength" of the attractive interaction between spherical particles with sticky interfacial interactions is defined by a phenomenological "stickiness parameter", τ. Since the direct experimental measurement and the physical interpretation of the parameter τ is problematic, Douglas and coworkers [23] directly related k_H to the second osmotic virial coefficient B_{22}, which is a well-known experimental metric of interparticle interaction based on the same sticky sphere frameworks of both Baxter and Russel [20,22]. The second virial coefficient B_{22} within this model is defined as

$$B_{22} = B_{22,ex} + \frac{1}{2} \int_{d_p}^{\infty} \left[1 - e^{(-\beta w(r))} \right] 4\pi r^2 dr \tag{3}$$

where "*ex*" denotes the purely repulsive excluded volume (hard sphere, *HS*) contribution. Note that for hard spheres, we have the simple geometric result, $B_{22,HS} = V_{ex}/2 = (2\pi/3) d_p{}^3$, where V_{ex} and d_p denote excluded volume and sphere diameter. $\beta^{-1} = k_B T$ where k_B and T denote Boltzmann's constant and absolute temperature, respectively, and $w(r)$ is the potential of mean force, i.e., the averaged force between a pair of molecules vs. radial separation, r.

With general equation of state ideas in mind as a potential framework for extending the application of this type of coarse-grained model to describe systems of interest in practical applications, B_{22} can be normalized by the steric contribution limit for mAbs to make this property dimensionless ($\Psi \equiv B_{22}/B_{22,ST}$). Then, this reduced virial coefficient Ψ can be used to enable a direct comparison of model predictions to measurements without any *adjustable parameters*. In particular, Douglas and coworkers [23] noted that Russel's result for k_H can be re-expressed in terms of Ψ as follows,

$$k_H = 3.42 - 2.43\,\Psi \tag{4}$$

This expression is a natural extension of a previously derived linear relationship [24,25] between the leading order hydrodynamic virial k_D coefficient for the collective diffusion coefficient D_c and Ψ. This quantity likewise provides a basic measure of solution interparti-

cle particle and is also currently being intensively investigated as a potential predictive measure of the stability of antibody solutions against aggregation [26,27].

Equation (4) highlights the fact that attractive interparticle interactions exist when the proteins are near their theta point at which $B_{22} = 0$ increases k_H ($\Psi = 0$) by roughly a factor of 3 in comparison to the case of hard spheres modeling the case of "good solvent" where the interparticle interactions are purely repulsive interactions, i.e., $\Psi = 1$. We note that Batchelor's hard sphere result [21,28], k_H ($\Psi = 1$) = 0.99 is recovered by Equation (4) so that Equation (4) is consistent with this classic colloid theory result. Many past studies have assumed spheres with a short range "sticky" attraction might provide a "universal" model of suspended particles systems with attractive interactions, including colloidal particles, polymers, and biological macromolecules such as proteins. Below, we also compare our results to another coarse-grained model of proteins that emphasizes that proteins are after all polymers of amino acids rather than spherical particles, and we compare to existing theoretical and measurement results for flexible polymers having a short-range attractive interaction defined in terms of Ψ, where the size is defined in terms of the polymer radius of gyration. Before proceeding to describe our experimental observations on model antibody solutions and compare our findings with the expectations of the sticky sphere and flexible chain models of proteins, we discuss the inherent limitations of these rather simplistic coarse-grained protein models and the qualitative physical origin of the interprotein interactions that make protein characterization highly challenging from both theoretical and technological viewpoints. The sticky sphere and flexible chain models of antibody proteins can only be considered stepping-stones to a more adequate theoretical framework of antibody solutions.

Brief Overview of the Complexities of Protein–Protein Interactions and Protein Association

We emphasize at the outset that both the idealized colloidal sphere and polymer models of antibody protein solutions should be viewed with some skepticism and, indeed, our observations on antibody protein solutions below indicate that this skepticism is well-justified. Many authors have previously reported the tendency of antibody proteins to dynamically associate in solution, which is a phenomenon that directly impacts the shear viscosity and other properties of these solutions [6,8,29–32]. These increases in viscosity with increasing protein concentration depend on the temperature, protein concentration, buffer excipients, pH, and other general "solution conditions".

We will discuss below observations indicating that there is a general tendency of proteins, as a class, to form supramolecular clusters [33–38], along with accompanying strong changes in the solution viscosity. This phenomenon cannot be understood from a simple colloid sphere model with a sticky interaction or neutral polymer model. Given the importance of this phenomenon for understanding the solution properties of antibody solutions, and protein solutions broadly, some explanation of the physical factors contributing to protein clustering seems warranted, and we devote this section to this matter.

While the biological community has long been concerned with a wide range of variables that complicate our understanding and prediction of inter-protein interactions [39–42], it is easy to identify the greatest shortcoming of the simple colloidal sphere and neutral flexible polymer models of proteins. Regardless of whether proteins are in the globular form of some globular proteins or take the form of swollen flexible polymer chains that are characteristic of intrinsically disordered proteins, protein molecules are most fundamental chains of amino acids, which are *dipolar molecules.* Moreover, protein molecules have macrodipoles, whose magnitudes tend to be especially large for proteins whose biophysical functionalities depend on their capacity to form strong molecular associations. In particular, dipole moments on the order of 1000 Debye (*D*) are rather common [43–48] in strongly associating proteins, while values on the order of 100 Debye are more typical of globular proteins whose function does not normally involve large scale supramolecular organization. Many proteins, including monoclonal antibodies, which bind to other "ligands" as part of their functional activity, lie in the middle range of this extremely wide range of dipole

moment values, and we may expect this range to be representative of antibody proteins, since they also bind to receptor targets expressed on/by cells. Antibodies form strong ligand–receptor complexes as part of their bio-activity (potency), and they are also intermediate structurally between globular proteins and denatured proteins that structurally resemble random coil polymers.

Van Workum and Douglas [47,48] have argued that dipolar, and sometimes strong quadrupole interactions, as in the case of tubulin and other sheet-forming proteins, are the primary interactions governing protein self-assembly where hydration-related relatively short-range interactions also play an important role in stabilizing the supramolecularly-assembled linear and branched polymer chain structures, membrane-like sheets, and closed "nanotube" and shell-like or "capsid" structures that naturally form this delicate balance between long-range directional and short-range attractions [47,48]. These dipolar interactions have been shown to have significant implications for the phase stability of solutions of dipolar particles [49] and protein solutions, by extension. The recognition of the predominant importance of dipolar interactions in protein and polypeptide solutions is not new. Brant and Flory noted that each amino acid group should contribute about 3.5 D to the polypeptide macrodipole [50], and later, other researchers emphasized the importance of protein macrodipoles in stabilizing protein structure [51,52] by influencing ion association and disassociation. We also mention the highly relevant work of Kirkwood and Shumaker [53,54], Antosiewicz and Porschke [46], and the more recent work by Adzic and Podgornik [55], which all emphasize the importance of charge and dipole fluctuations in contributing to the observed effective macrodipole interactions of proteins. These works make it clear that knowledge of protein structure is not sufficient to specify the multipole interactions of proteins in solution, which can rather complicate theoretical modeling of these solutions. Minimally, the protein and ion association must be modeled to account for these charge fluctuation effects, which means that solvation effects must be accounted for in the modeling.

Based on these general considerations, it should come as no surprise that recent experimental studies of dipole–dipole interactions in antibody solutions have revealed a strong correlation between the antibody dipole moment, which can depend appreciably on pH, and the macroscopic viscosity of the antibody solution. This has led to a general recognition of the importance of these interactions [34,56], and this knowledge has also led to successful efforts at developing additives that modulate the dipolar interactions in order to inhibit the protein self-assembly process for clinical applications relating to antibody drug delivery [31]. This knowledge appears to offer a very promising conceptual framework for engineering improved antibody formulations.

Then, the measured viscosity of protein solutions depends on the number of proteins in these aggregates, their polydispersity and size, as well as whether there is a persistence of their aggregated state. We are clearly dealing with a very complex class of materials. As noted before, protein clustering is particularly natural in antibody protein solutions because of their prevalent dipolar interactions. This is the real problem that we are up against in our effort to establish a general metric for quantifying interparticle interactions strength in protein formulations. In previous work [14], we pointed out clear evidence for the inadequacy of modeling proteins as spherical particles with short-range sticky interactions, and we then suggested that we should address the inherently polymeric nature of proteins. The findings of the present work imply that we must consider multipole interactions or at least the directional aspect of such interactions in any minimal model of the protein solutions. Attempts to model such interactions are ongoing, and briefly, we outline some recent promising attempts to address this type of interaction.

Recent simulation studies have begun the ambitious task of incorporating such interactions [57] into molecular dynamics of protein solutions, but this effort requires the incorporation of explicit solvent to address ion and protein solvation phenomena [58] and will require large-scale simulations. Despite these complexities, we may gain some qualitative insight into protein assembly from the Stockmayer fluid [47], which is a minimal

model of proteins in solution that combines a particle dipole–dipole interaction with a competitive van der Waals interaction, as described by the well-known Lennard–Jones interaction. When the dipole–dipole interaction strength is strong [47,48], the particles in this model exhibit a large degree of reversible self-assembly into linear polymer chains whose size depends on temperature, particle concentration, and other thermodynamic physical factors, as found in found in previous studies of amyloid protein self-assembly of amyloid fibrils [59–62] and actin polymerization under equilibrium conditions [63–65]. Exact analytical calculations of B_{22} of the associating particles in the Stockmayer model fully account for their reversible associations [47] through their renormalization of the second virial coefficient. Van Workum and Douglas [47,48] have explained why the Stockmayer model, which includes competitive van der Waals and dipolar interactions, and its quadrupolar interaction generalization, are highly attractive general coarse-grained models for protein self-assembly that address their strong dipolar and quadrupolar interactions [47,48], and they also describe their corresponding general tendency to self-assemble into dynamic polymeric structures. Then, we have some hope that aggregating particle systems exhibiting weak but reversible self-association might be described phenomenologically by this type of highly coarse-grained protein model that accounts for the highly directional interactions that are intrinsic to proteins and many other biological and synthetic supramolecular assembling molecules [66].

There are also some coarse-grained models that neglect the long-range nature of the multipole interactions for computational expediency. In particular, the long-range multipole interactions are replaced by "sticky" spots on the surface of a spherical particle modeling the protein, so we return again to what could be called a colloidal protein model. In particular, this type of highly coarse-grained protein model has been found to be useful in gaining insights into the phase separation of protein solutions [17,19,67–70]. Recent work has adapted this type of "spot model" to describe antibody proteins based on an extension that replaces the individual sphere with spots by small polymers of beads that have spots in which the polymers form a Y-like configuration (a star in polymer science parlance) that is characterized by the geometrical structure of real antibodies in solution. This is a somewhat more elaborate but still highly coarse-grained model of antibodies in solution that has allowed the quantitative estimation of the polymer cluster size distributions, the Huggins coefficient, and the second osmotic virial coefficient over a wide range of thermodynamic conditions [71]. This model, and the related model of Skar-Gislinge et al. [72], have not yet been shown to quantitively agree with measurements. This type of modeling is still a work in progress, but this approach seems very promising.

In another important development, the sticky spot model has been extended to include an explicit solvent and counterions [71]. An extension of the antibody model to incorporate such hydration-related physics would probably go a long way toward having a coarse-grained model of predictive value for predicting at least trends in antibody solution properties if the parameters in the model were carefully determined through a synergistic comparison between simulation and measurement efforts on protein solutions. Hofmeister specific ion effects associated with ion hydration are implicated in a wide range of biological phenomena, including protein binding and stability [58], and as general factor relevant to excipient additives [73] for antibody formulations to improve their solution [74,75]. The general lack of understanding of Hoffmeister and other protein and ion hydration effects is perhaps the weakest link in all existing methods aimed at modeling the properties of protein solutions, while at the same time, these effects offer great opportunities for practical applications for enhanced antibody solution stabilization and an enhanced knowledge of aqueous solutions broadly.

Another basic, and related, problem is that molecular flexibility [76,77], which is influenced by hydration, molecular structure, ion association, and many other factors, makes an often large contribution to the entropy of binding and thus the overall binding affinity [78,79]. The relation of antibody rigidity in the regulation of molecular binding strength has been especially studied in antibodies because their rigidification occurs rapidly

in the course of the "maturation" of the binding affinity to the antigen's final "evolved" value [80–82]. This same process seems to be involved for conserved proteins and their fundamental binding processes in the adaption of organisms to different environments [79]. A general lack of understanding of how rigidity influences molecular binding in aqueous solutions is a central problem that has often prevented the successful prediction of molecular binding constants of protein-based drugs [83–85].

There is ongoing work to develop an effective minimal model of antibody solutions that involves just enough "coarse-graining" of the protein solution physics, along with a measurement program to establish basic trends in the model parameters of such a theory to enable the organization and interpretation of the rapidly growing number of measurements in this critically important class of materials for human health. Such a model should be useful to the biopharmaceutical community in the rational design of stable antibody formulations optimized in terms of efficacy, safety, and economic costs for their intended clinical use.

While we are waiting for the development of an effective theory of the properties of antibody solutions, we feel that a focus on B_{22} and on corresponding properties greatly dependent on B_{22}, such as k_H, and the corresponding virial for the collective diffusion coefficient k_D [26,27] might provide rational metrics for characterizing inter-protein interaction strength under conditions where near-equilibrium association and relatively good dispersion prevails. This ultimate goal transcends whether the protein data itself quantitively 'fit' the theoretical predictions of the coarse-grained model. Protein solutions exhibiting a high degree of irreversible association ("aggregation") are excluded from our current consideration because of the highly negative immune response that such solutions would trigger upon administration to patients. Therefore, the systems studied have been "selected" to eliminate cases of irreversible protein aggregation.

2. Materials and Methods

Broadly neutralizing monoclonal antibodies "mAb-1" [86], "mAb-2" [87], and "mAb-3" [88] (Table 1), targeting the CD4-binding region of human immunodeficiency virus 1 (HIV-1), are in development by the National Institutes of Health (NIH) Vaccine Research Center (VRC) for clinical research. Their F_{ab} crystal structures and primary amino acid sequences are available in the Protein Data Bank (PDB). To retain their unique biological activities, the sequence of the mAbs were minimally optimized for stability. The antibodies were expressed by Chinese Hamster Ovary (CHO) cells, purified by protein A chromatography followed by a polishing step consisting of ion exchange resin chromatography, and then concentrated in their respective formulation buffer to 100 mg/mL nominal protein concentration (Table 1). All IgG solutions were stored at $\leq -65\,°C$, thawed immediately before use, and filtered via 0.22 μm polyvinylidene fluoride (PVDF) syringe filters prior to measurements.

For the pH-dependence studies, mAb-3 stock solution at 40 mg/mL was dialyzed against 20 mM histidine-acetate buffer at $4.2 \leq pH \leq 6.2$, using Slide-A-Lyzer™ dialysis cassettes with a molecular weight cutoff of 20,000 (ThermoFisher Scientific, cat. # 66012, Waltham, MA, USA). Following dialysis, pH was confirmed, and samples were formulated with the required NaCl. All buffer components were compendial USP grade for high purity (VWR Avantor, Radnor, PA, USA).

Table 1. Monoclonal antibodies (mAbs) and formulation buffer compositions.

Antibody	PDB ID	Molar Mass (*kDa*)	Protein Iso-Electric Point Main Peak/Range	Buffer Composition	Net Ionic Strength (mM)
mAb-1	4LST	148	9.06; 8.78–9.25	25 mM Na citrate, 50 mM NaCl,150 mM arginine HCl, pH 5.8	278.8 *
mAb-2	5FYJ	151	9.30; 9.14–9.59	50 mM histidine HCl, 50 mM NaCl, 5 % (*w/v*) sucrose, 2.5% (*w/v*) sorbitol, pH 6.8	56.9
mAb-3	5TE4	158	9.13; 8.99–9.47	10 mM Na citrate, 50 mM NaCl 150 mM arginine HCl, 0.002% (*w/v*) polysorbate 80, pH 6.5	246.3
mAb-3 (pH Variation)	5TE4	158	-	20 mM histidine acetate, 50 mM NaCl $4.2 \leq pH \leq 6.2$	70 †

* Assuming arginine hydrochloride is in +1 state, which should be accurate. † 20 mM histidine-acetate buffer was prepared by mixing the pure solid histidine base with liquid acetic acid, and the ionic strength from the buffer is always 20 mM, since no other counterions were introduced into the system. Detailed calculations of ionic strength are provided in Supporting Information.

2.1. Size Exclusion Chromatography (SEC)

Immediately prior to testing, mAb samples were diluted with 2X PBS to 1 mg/mL. Fifty μg of mAb was injected onto the Waters Acuity^{TM} BEH (ethylene bridged hybrid, Waters, Milford, MA, USA) SEC column (P/N: 186005225; 4.6 mm × 150 mm I.D, particle size: 1.7 μm, pore size: 20 nm) of the Waters Acuity UPLC H-Class system (Waters, Milford, MA, USA). An isocratic 2X PBS mobile phase (pH 7.4) was run at a flow rate of 0.4 mL/min for 6 min. UV absorbance was detected at 280 nm using Empower 3 software (Waters, Milford, MA, USA). The percentage monomer, aggregate, and fragment for each system was determined by integration of the area under the peak of UV signal vs. elution time. Only one SEC injection/measurement was performed for each sample, as is typically done.

2.2. Capillary Iso-Electric Focusing (cIEF)

Capillary Isoelectric Focusing utilizing the iCE3 platform (IEF, PrinCE micro injector auto sampler, iCE 3 software package v. 3.0 and Chrom Perfect iCE3analysis software v. 6.0.4; ProteinSimple, San Jose, CA, USA) is an assay used to evaluate the charge heterogeneity of charged isoforms of proteins. cIEF is a charge-based separation technique that separates molecules based on their isoelectric point (pI). Samples are prepared by mixing the protein of interest with selected carrier ampholytes and pI markers. Then, the samples are loaded into the capillary cartridge (cIEF cartridge FC-coated (ProteinSimple, San Jose, CA, USA, Cat # 101701). Acid and base are added to the electrolyte tanks on the cartridge, and a voltage is applied in which analytes are focused at their pI. The focusing step is captured in real time by a charge-coupled device (CCD) camera, which takes a picture of the entire length of the capillary column every 30 s. The resulting separation is an electropherogram that identifies the pI and absorbance of the protein peaks. The samples comprised 50 μL of 2 mg/mL mAb, 100 μL of master mix solution, 150 μL of ultra-pure water. Each single mL of master mix solution comprised 740 μL of 1% Methyl Cellulose Solution, 200 μL of 8–10.5 ampholyte, and 20 μL each of 3–10 ampholyte, pI standard 7.9, and pI standard 10.1. The focusing times in focus periods 1 and 2 were 3.0 and 10.0 min, respectively, while the voltages in focus periods 1 and 2 were 500 and 3000 V, respectively.

2.3. Viscometry

Samples were prepared from 100 mg/mL stock mAb solutions and diluted between 0.1 and 90 mg/mL in their respective buffers. Concentrations were confirmed by UV/Visible spectroscopy (Agilent 8453 UV-Visible spectrophotometer, Agilent Technologies, Santa Clara, CA, USA) using gravimetric dilutions.

Solution η of mAbs was measured using the Viscosizer (Malvern Panalytical, Malvern, UK). Measurements were performed at 25 °C using an uncoated fused silica capillary, with an inner diameter of 75 μm and 130 cm total length. Air-driven viscosity measurements

were performed at a constant pressure differential of 3000 mbar, which translated to shear rates between 1300 and 4600 s^{-1}. The measured viscosity was independent of shear rate for all solutions.

2.4. Osmotic Second Virial Coefficient Determination

Static light scattering (SLS) was used to determine the osmotic second virial coefficient (B_{22}). Samples were prepared from 100 mg/mL stock solutions by gravimetric dilution to 2, 4, 6, 8, and 10 mg/mL with their respective buffers. SLS measurements were performed using a high-throughput fluorimeter/scattering system (UNcle, Unchained Labs, Pleasanton, CA, USA). Each measurement was conducted at 25 °C and consisted of 10 acquisitions of 30 s each, with laser power and attenuation set to 100% and 25% respectively. The excess Rayleigh scattering ratio, Kc_2/R_θ, was determined from 660 nm wavelength data. Employing classical Debye–Zimm analysis [89], the B_{22} values were determined from the slope of the Debye–Zimm plot. National Institute of Standard and Technology (NIST) mAb Reference Material 8671 (NIST, Gaithersburg, MD, USA) was used as an absolute reference standard for SLS to determine the light scattering constant K, which assumes that the refractive index increments (dn/dc) for each antibody solution are similar to each other.

2.5. Hydrated Protein Molecular Volume: Atomistic Monte Carlo Computer Simulations

Antibody molecular volumes, v_2, were calculated by simulating the virial coefficient B_{12}, which quantifies protein–water interactions; subscripts 1 and 2 denote water (solvent) and protein (solute), respectively. In the limit where only steric interactions (*ST*), i.e., excluded volume effects, are present, $2B_{12,ST}$ is an estimate of the excluded volume of protein with respect to a single water molecule approximated as a solid sphere of diameter 0.3 nm (the pre-factor 2 comes from the derivation in Equation (5), due to the $\frac{1}{2}$ pre-factor). This is equivalent to the total volume of water that will be excluded from the protein molecule in solution. Since proteins are expected to always carry at least one solvation layer, due to the energetic penalty of disrupting such a layer, $2B_{12,ST}$ is a perfect estimate of the protein-excluded volume.

$B_{12,ST}$ was computed using the Mayer Sampling with Overlap Sampling (MSOS) algorithm [90] for an all-atom description, including hydrogens, of a generic mAb with variable F$_{ab}$ regions, taken using PDB F$_{ab}$ and generic PDB 1IGT F$_c$ (fraction crystallizable) crystal structures. The MSOS algorithm efficiently solves the equation of B_{12} for purely steric interactions [91,92]. The contribution from the antibody hinge regions is small, $\approx$ few %, based on the total number of amino acids there, and hence, it was neglected as an engineering approximation:

$$B_{12} = -\frac{1}{2} \int \int \int_{r\Omega_1\Omega_2} \left[e^{\left(-\frac{w_{12}(c_{1,2}\to 0,\ r,\Omega_1,\Omega_2)}{k_B T}\right)} - 1 \right] dr d\Omega_1 d\Omega_2. \tag{5}$$

The detailed method of evaluation of Equation (5) is described in Refs. [91,92] Several simulations of $B_{12,ST}$ as a function were performed for an assumed water hydration layer thickness σ_w in a range, 3 nm $\leq \sigma_w \leq$ 7 nm. A linear extrapolation to the limit $\sigma_w = 0$ nm for the mAbs investigated indicates a specific volume estimate, $v_2 \cong 1.14 \pm 0.03$ mL g^{-1}, if v_2 is equated with $2B_{12,ST}$ in the $\sigma_w \to 0$ limit. Figure 1 shows this extrapolation procedure for mAb-1.
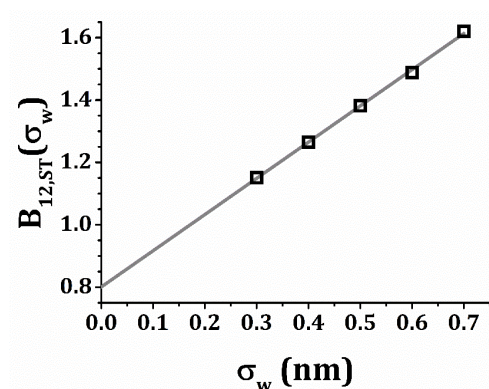
Figure 1. Computed steric contribution to the virial coefficient, B_{12}, plotted vs. protein hydration layer thickness, σ_w. The points are computed data; the line serves as a visual guide for the extrapolation.

3. Results

3.1. Biophysical Characterization

Size Exclusion Chromatography (SEC)

The ratio of monomer and aggregate content in solution is well appreciated in determining the shear viscosity of protein and antibody solutions, which necessitates the need to make SEC measurements [8,16,93,94]. Therefore, solution SEC data at 25 °C are provided in Table 2. The IgG molecules are mostly in the monomeric state (97.0%) in the mobile phase buffer solution. There is a notable drop in the monomer content for mAb-3 at pH 6.2 to 95.8%. These SEC data will be invoked further during a discussion of the Huggins coefficient data.

Table 2. Size exclusion chromatography (SEC) data on monoclonal antibodies.

System	% Monomer	% Fragment	% Aggregate
mAb-1 formulation	99.0	0.0	1.0
mAb-2 formulation	98.0	0.0	2.0
mAb-3 formulation	99.0	0.0	1.0
mAb-3 pH 4.2	98.8	0.4	0.8
mAb-3 pH 4.5	98.6	0.3	1.1
mAb-3 pH 4.9	97.8	0.2	2.0
mAb-3 pH 5.4	97.8	0.0	2.2
mAb-3 pH 5.9	97.1	0.0	2.9
mAb-3 pH 6.2	95.8	0.0	4.2

3.2. Antibody Solution Viscosity and Its Reduction

Solution η data at 25 °C vs. c_2 are plotted in Figure 2. The inset plot of dimensionless η_R vs. dimensionless c_2 $[\eta]$ in Figure 2 collapses data for different mAbs in their formulation buffers at low protein concentrations onto a single curve, as is commonly observed in polymer solutions under fixed solvent quality conditions [95]. In such an "equation of state data reduction" [96], the solution concentration is conventionally rendered dimensionless using the intrinsic viscosity, which defines a hydrodynamic volume. The breakdown of this reduction occurs near the "overlap concentration", which is defined by the condition, c_2 $[\eta] \approx 1$. The lack of η_R data superposition in this figure when c_2 $[\eta] > 0.1$ is due to the variable solvent quality of the different antibody formulations, and we then expect k_H to quantify the non-ideality of these inter-protein interactions. The values of k_H and $[\eta]$ extracted from non-linear least squares regression fits of η_R vs. c_2 to Equation (2) (Figure 3) are provided in Table 3. The magnitude of k_H in these mAbs agrees well with values reported by Yadav et al. [97] for other mAbs: $1.5 \leq k_H \leq 6.6$ and $[\eta] \approx 6$ mL/g. Values in this range have been reported in charged biopolymer systems, but these values exceed estimates reported for uncharged flexible polymers [98,99]. This observation provides an

important clue that long-range interactions are relevant to understanding the k_H values of these antibody solutions.
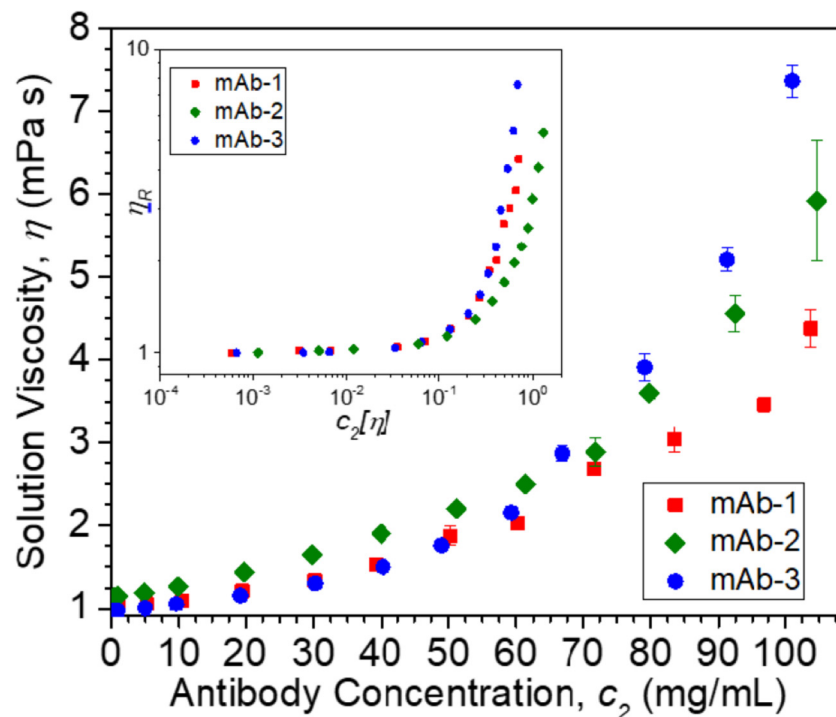

Figure 2. Viscosity η at 25 °C vs. mass concentration units (c_2) of mAb formulations. Inset shows relative viscosity η_R plotted vs. dimensionless concentration c_2 [η]. Bars on data points denote standard deviations. Note that mAb-2 buffer contains 5% (w/v) sucrose and 2.5% (w/v) sorbitol, resulting in higher η values than mAb-1 and mAb-3 buffers. For both mAb-1 and mAb-2, each data point was an average of $n = 3$ measurements, while for mAb-3, each data point was an average of $n = 5$ measurements.
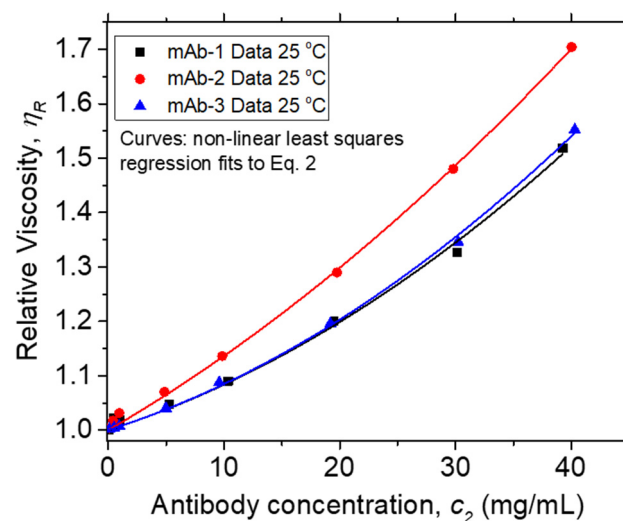

Figure 3. Relative viscosity η_R at 25 °C vs. mass concentration units (c_2) of Vaccine Research Center (VRC) mAbs. Points and curves denote data and non-linear least squares regression fits to Equation (2), respectively. R^2, values for fits to mAb-1, mAb-2, and mAb-3 data are 0.999, 0.992, and 0.999, respectively.

Table 3. Experimentally determined values of Huggins coefficient k_H, intrinsic viscosity $[\eta]$, and osmotic second virial coefficient B_{22} at 25 °C for mAbs.

Antibody in Buffered Formulation	Huggins Coefficient, k_H [2,3,4]	Intrinsic Viscosity $[\eta]$, mL/g [1,2,4]	$[\eta]$ Volume Fraction Units	$\Psi \equiv B_{22}/B_{22,ST}$ [1,5]
mAb-1	3.3 ± 1.6	6.8 ± 1.0	6.0 ± 0.9	0.47 ± 0.14
mAb-2	0.9 ± 0.2	12.4 ± 0.7	10.9 ± 0.6	0.50 ± 0.13
mAb-3 (at fixed pH 6.5)	3.6 ± 0.8	6.8 ± 0.5	6.0 ± 0.4	0.68 ± 0.15

[1] B_{22} was normalized as $B_{22}/B_{22,ST}$, and $[\eta]$ was made dimensionless by dividing it by v_2. [2] k_H and $[\eta]$ were determined from fits of Equation (2) to η_R data limited to $\phi_2 \leq 0.06$, where the virial expansion remains valid. [3] Note that k_H is dimensionless in reduced c_2 $[\eta]$ units. [4] The uncertainty ($\pm$) in k_H and $[\eta]$ was extracted from the non-linear least squares regression fits based on the Levenberg–Marquardt algorithm. [5] $B_{22,ST}$ values calculated for immunoglobulin 1 (IgG1) mAbs were taken from Grünberger et al. [100] and Calero-Rubio et al. [91,101].

Intrinsic viscosity $[\eta]$ measurements are difficult to perform accurately, and there are correspondingly appreciable uncertainties in Huggins coefficient k_H estimates in all studies, even including model systems such as near monodisperse uncharged flexible synthetic polymers in organic solvents [98]. Therefore, we have applied two common methods of estimating k_H to check on the consistency of our estimations under these circumstances–the "Huggins Equation",

$$\frac{\eta_{sp}}{c} = [\eta] + k_H [\eta]^2 c \tag{6}$$

And virial expansion (see Equation (2) and non-linear regression fits in Figure 3). The results from both these approaches agree within experimental uncertainties, and this fact provides greater confidence in the numerical estimation of both $[\eta]$ and k_H. The detailed results are provided in the Supporting Data for this manuscript.

In addition to measurements of the viscosity of each antibody in its respective formulation buffer, the viscosity of mAb-3 was measured as a function of pH, because pH is an important solution property that sets the net charge on protein molecules and affects their conformation as well as protein–protein interactions. The η_R vs. c_2 data for mAb-3 solutions across the pH range $4.2 \leq \text{pH} \leq 6.2$ and non-linear regression fits to Equation (2) are shown in Figure 4. The histidine-acetate buffering system chosen here allows a precise control of pH over small pH changes across this pH range. The values of k_H and $[\eta]$ extracted from non-linear least squares regression fits of Equation (2) to the data are provided in Table 4.

Table 4. Huggins coefficient k_H, intrinsic viscosity $[\eta]$, and the normalized osmotic second virial coefficient B_{22}, i.e., $M\, B_{22}/B_{22,ST}\, [\eta]$, at 25 °C for mAb-3.

mAb-3 Solution pH	Huggins Coefficient, k_H [1-3]	Intrinsic Viscosity $[\eta]$ (mL/g) [1,3]	$[\eta]$ Volume Fraction Units	$\Psi = B_{22}/B_{22,ST}$
4.2	2.1 ± 0.3	7.7 ± 0.3	6.8 ± 0.3	1.25 ± 0.26
4.5	7.6 ± 3.1	5.4 ± 0.8	4.7 ± 0.7	1.15 ± 0.31
4.9	5.6 ± 2.7	7.1 ± 1.3	6.2 ± 1.1	0.68 ± 0.18
5.4	5.2 ± 2.7	6.7 ± 1.2	5.9 ± 1.0	0.57 ± 0.14
5.9	2.4 ± 1.7	9.0 ± 1.9	7.9 ± 1.7	0.48 ± 0.11
6.2	3.8 ± 1.9	7.2 ± 1.2	6.3 ± 1.1	0.53 ± 0.50

[1] Both k_H and $[\eta]$ were determined from fits of Equation (2) to η_R data for the concentration range $\phi_2 \leq 0.06$, where the virial expansion is valid. [2] Note that k_H is dimensionless in reduced c_2 $[\eta]$ units. [3] The uncertainty ($\pm$) in k_H and $[\eta]$ was extracted from the non-linear least squares regression fits based on the Levenberg–Marquardt algorithm.
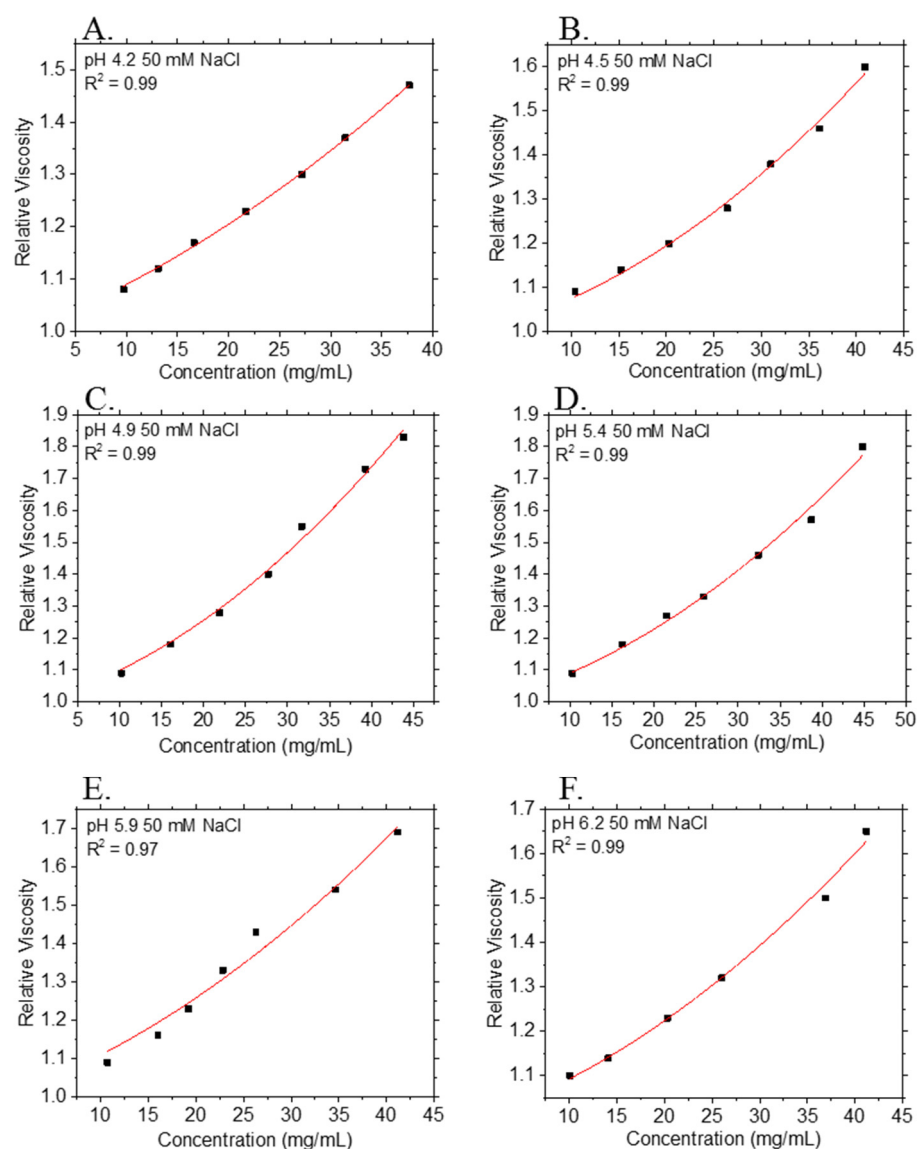
Figure 4. Relative viscosity η_R at 25 °C vs. mass concentration (c_2) of mAb-3 formulation in buffers having a range of pH values: **(A)** pH = 4.2; **(B)** pH = 4.5; **(C)** pH = 4.9; **(D)** pH = 5.4; **(E)** pH = 5.9; **(F)** 6.2. Points and curves denote experimental data and non-linear least squares regression fits to Equation (2), respectively. R^2 values for fits are provided in the legends. Each data point is an average of $n = 5$ measurements, except for data at pH = 5.9: each data point is an average of $n = 3$ measurements. Although no error bars are displayed, all data points have a percentage relative standard deviation of <5.0%.

Unsurprisingly, our k_H estimates on pH provide further evidence of charge interactions in our protein formulations. The isoelectric point (pI) of mAb-3 is ≈ 9.0; as the $|\text{pI} - \text{pH}|$ increases, the surface charge on the mAb increases, resulting in increased electrostatic repulsion between the protein molecules. As seen in the mAb-3 samples at various solution pH, a lower pH results in Ψ values greater than unity. This trend is also expected for objects that that are asymmetric in shape and interact with each other through repulsive interactions. It is clear from Table 4 that $[\eta]$ in volume fraction concentration units is larger than the classical Einstein hard sphere value[30] of $[\eta] = 2.5$. For mAb-3, any pH dependence of $[\eta]$ is hard to discern, given the uncertainty in estimation of $[\eta]$ at some of the pH values, even though the correlation coefficient R^2 is ≥ 0.97 for the fits to the η_R data. Together, these results point to the importance of particle shape on these virial coefficients and the limitations of the idealized hard sphere model of proteins that pervades the literature.

These conclusions are qualitatively in accord with the messages from a previous paper by a subset of the authors [14,102].

4. Discussion

Comparison of Antibody Solution Measurements with Flexible Polymer and Sticky Sphere K_h Models

To better motivate a discussion of Huggins coefficient in terms of idealized colloidal and polymer models of antibodies and the consequent comparisons to molecular theories, a review of the definitions for conventional concentration units used in polymer and colloid science and issues related to the inter-conversion between these units is warranted. In polymer and protein science, it is conventional to measure the macromolecule solute concentrations c_2 in units of g of macromolecule/mL solution. Then, the solution viscosity η is described by the same power series expansion as in Equation (2).

$$\eta_R = \eta / \eta_s = 1 + [\eta]\, c_2 + k_H\, ([\eta]\, c_2)^2 + \ldots \tag{7}$$

Here, $[\eta]$ correspondingly has units of mL/g, because η_R is dimensionless, by definition. It is also traditional in polymer science to introduce reduced concentrations defined in terms of a polymer "overlap concentration" [89] c^*, at which inter-polymer interactions start to become appreciable. Specifically, Equation (7) is formally re-written as,

$$\eta / \eta_s = 1 + (c_2/c^*) + k_H\, (c_2/c^*)^2 + O(c_2/c^*)^3, \tag{8}$$

where the overlap concentration that signifies the onset of inter-polymer interaction is defined as $c^* = 1/[\eta]$. The chain radius of gyration R_g may also be used to define dimensionless concentration units for polymer solutions based on the concept of geometrical overlap [103,104], but dynamical properties such as η are usually defined in terms of $[\eta]$. Note that k_H is theoretically invariant to the choice of concentration units, although the conversion between mass concentration units to volume fraction units can give rise to uncertainties associated with estimating the protein molecular volume. As will be discussed below, k_H in polymers typically ranges from about 0.7 in a good solvent where excluded volume repulsions are strong, as in solutions of hard spheres, to a value near 0.3 in a θ solvent where attractive interparticle interactions between the polymers exactly balance the repulsive interactions in B_{22}, i.e., $B_{22}\, (T = T_\theta) = 0$ [13]. This "ideal" or "θ point" state for solutions of polymers or particles at which interparticle excluded volume interactions effectively vanish is the exact analog of the Boyle temperature, T_B, in non-ideal gases [13,105].

The viscosity virial expansion for suspensions of hard sphere Brownian particles is naturally described in terms of a virial expansion in terms of volume fraction [106,107].

$$\eta / \eta_s = 1 + 2.5\, \phi_2 + 6.2\, \phi_2{}^2 + O(\phi_2{}^3) = 1 + 2.5\, \phi_2 + k_H\, (2.5\, \phi_2)^2 + O(\phi_2{}^3) \tag{9}$$

The leading term 2.5 pre-factor is due to Einstein [108] and the second-order viscosity virial coefficient 6.2 is due to Batchelor[14]. The "O" symbol denotes "order of magnitude". As noted before, k_H for the sticky hard sphere model, where there is a variable short-range attractive interaction, is given by Equation (4). Then, we may deduce the repulsive hard sphere estimate for the Huggins coefficient, $k_H \approx 0.99 \approx 1.0$, by inserting $\Psi = 1$ in Equation (4).

Then, these colloidal estimates can be compared with the theoretical estimate of k_H for flexible polymer solutions in a θ solvent, $k_H\, (\Psi = 0) \approx 0.757$ derived by Edwards and Freed [109] and the good solvent estimate $k_H\, (\Psi = 1) \approx 0.4$ of Muthukumar and Freed [110]. Yamakawa [111] derived an expression for k_H covering intermediate degrees of excluded volume interaction strength, $0 < \Psi < 1$, which can be approximately expressed as $k_H \approx \frac{1}{2} - 0.3\, \Psi$, corresponding to a variation between 0.5 and 0.2 upon going from θ solvent to a good solvent; the variation is nearly linear with the B_{22}, as suggested by the sticky sphere model variation of k_H. Classical measurements by Berry [99] on polystyrene

solutions support these theoretical predictions to a reasonable approximation, although the experimental estimates have tended to be a little smaller in magnitude than the theoretical predictions for k_H. Evidently, k_H for polymer solutions has a similar qualitative variation with "solvent quality" (Ψ) as for the stick sphere model, but the magnitude of k_H is significantly larger for hard sphere particles. This qualitative difference in the relative magnitude of k_H offers a chance to gauge whether antibodies resemble spherical colloidal particles or flexible polymers, and we next consider an estimate of k_H for our antibody solutions over a broad range of solvent quality.

The observation noted above brings us to a consideration of whether B_{22} measurements provide valuable insight into the change in η_R exhibited in Figures 3 and 4. B_{22} values of our mAb solutions were determined using SLS, and they were normalized by $B_{22,ST}$ to calculate Ψ. Grünberger et al. [100] and Calero-Rubio et al. [91,101] have calculated $B_{22,ST}$ for IgG1 mAbs: $B_{22,ST} \cong 10$ mL g^{-1}. The Ψ values for these mAbs (Tables 3 and 4) are $\cong$ 0.5–0.7, in contrast to NIST mAb, for which $\Psi = 1.99$ (NIST mAb $B_{22} = 19.9$ mL/g; personal communication from Vincent Shen and Marco Blanco-Medina, NIST, Gaithersburg, MD, USA) (If proteins were true hard spheres, then Ψ could not exceed 0.99, providing further evidence that antibodies cannot be described physically as hard spheres).

We obtain further insight into this situation through a consideration of recent osmotic pressure and scattering measurements of serum albumin solutions [112], where the properties of their protein solution were found to be consistent with a solution of oblate ellipsoids. If we accept this as being an acceptable "coarse-grained" model of our Y-shaped antibodies with a rough estimate of aspect ratio (5 × 1), then Ψ can be exactly computed to equal, Ψ (hard oblate ellipsoid; 1 × 5) = 1.89 [113].

If we simply ignore the obvious difficulty of treating antibodies as being hard sphere and plot k_H as a function of Ψ, then we may check whether at least the qualitative trends of sticky hard sphere and polymer models are followed. In Figure 5, we directly compare our antibody data for k_H vs. Ψ. Our observations indicate that there might be a general trend that k_H increases as ψ is reduced, but there is clearly no quantitative agreement with either the sticky hard spheres or polymer with variable excluded volume interaction models. Data for mAb-2 do approach the flexible polymer chain prediction, but the data for mAb-1 and mAb-3 clearly depart from the flexible polymer chain model. The pH-dependent data for mAb-3 do not even qualitatively agree with the flexible polymer chain model and the data for mAb-1, mab-2, and mAb-3 are also not well described by the adhesive hard sphere model estimate of k_H in terms of ψ introduced by Douglas et al. [23]. Meanwhile, the pH-dependent data for mAb-3 admittedly have appreciable uncertainty. Pamies et al. [98] have noted the challenges associated with the determination of $[\eta]$ and k_H by single-point and dilution procedures, and the large uncertainty associated with the determination of k_H; their lack of agreement with both the hard sphere and the flexible polymer chain models is an effect beyond this uncertainty. We note that the antibody solution model of Kastelic et al. [71] mentioned above also predicts that k_H varies linearly with Ψ, but the predicted variation of k_H appears to be much weaker than the colloid sphere model of Russel. In particular, Kastelic et al. find k_H to equal 0.6 near the theta point where Ψ vanishes, which is in the range (0.5, 0.57) of the estimates of k_H for the polymer model.

This deviation is understandable given the lack of consideration of charge, dipole interactions, hydration, and other factors known to contribute to protein–protein interactions in protein solutions. As seen in both Table 4 and Figure 5, under acidic pH conditions, Ψ for mab-3 is significantly larger than its theoretically maximum value for a repulsive hard sphere, i.e., $\Psi = 1.0$, which might be attributed to an increase in repulsive electrostatic interactions or perhaps some deviation from a spherical protein shape based on a simple colloidal sphere protein. However, the increasing trend in Ψ with lowering pH is not reflected in changes in the intrinsic viscosity values, which instead exhibit a minimum at pH 4.5. A simple change of protein shape simply cannot reasonably be invoked to rationalize the large value of k_H observed in our measurements. Accordingly, we interpret the large value of k_H to arise from a large dipole–dipole interaction, as discussed

above [31,34,56,97,114]. Of course, charge and dipolar interaction effects should also make a significant contribution [115] to B_{22}, but even under conditions of strongly repulsive protein–protein interactions, we still see a deviation from the colloidal sphere model, which would generally require $\Psi < 1$. We concur with other recent studies of antibody solutions noted above indicating the complete inadequacy of the hard sphere model of the solution viscosity and other solution properties of antibody protein solutions, including our past study coming to the same conclusion [14]. We must add to this conceptual pyre [102] the neutral polymer model of antibodies, which is also a clearly physically inadequate model of this class of proteins. Clearly, an improved understanding of protein hydration, ion solvation, and dipole–dipole, charge–dipole, and perhaps multipole interactions is required to fully understand the molecular significance of the viscometric interaction parameter k_H of antibody solutions. Despite these difficulties, k_H along with k_D [26,27] provides a useful practical measure of the strength of inter-protein interactions at elevated protein concentrations of direct significance to developing antibody formulations that minimize the solution viscosity for many clinical applications.
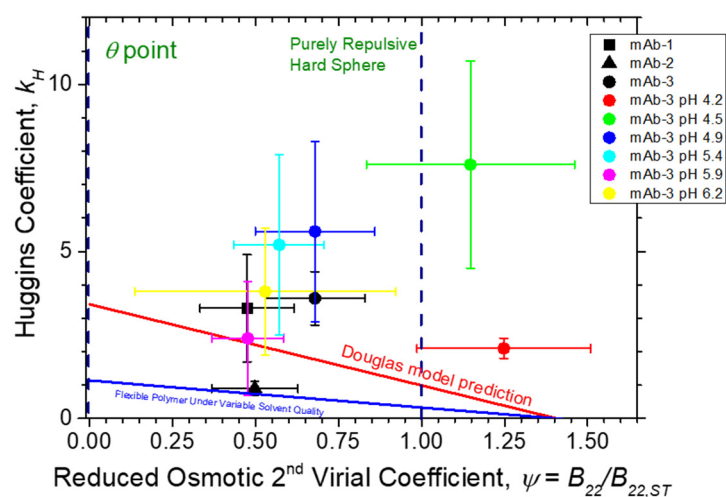
Figure 5. Huggins coefficient k_H vs. reduced osmotic second virial coefficient. Comparison of Ψ (circles) to Douglas et al. [23] model prediction (continuous red line; Equation (4)) and an estimate (see text for discussion) for flexible polymer chains with variable excluded volume interaction (continuous blue line). Uncertainty estimates were determined from the non-linear regression of Equation (2) to η data, and linear regression of Equation (6) to SLS Kc_2/R_θ data. Dashed vertical lines denote limiting k_H values at the θ point ($\Psi = 0$) and for purely repulsive hard spheres ($\Psi \approx 0.99$), respectively.

5. Conclusions

This work has provided the experimental measurements of Huggins coefficient, k_H, a classical measure of the interparticle interaction strength, for three monoclonal antibodies in solution. The intrinsic viscosity $[\eta]$ of these antibody solutions, a basic measure of macromolecular shape/conformation, was determined by using the relative viscosity data from classical capillary viscometry. The range of $6.0 \leq [\eta] \leq 10.0$ for these antibodies significantly exceeds the classical Einstein result of 2.5 for hard spheres, confirming that these antibodies do not behave as hard spheres. Another basic measure of inter-protein interaction, the second osmotic virial coefficient, B_{22}, was also measured using static light scattering with the objective of critically scrutinizing literature-proposed models of proteins, viz., the sticky hard sphere model and the flexible chain polymer model. The relative viscosity data for all the antibody solutions tested were reduced to a single curve by use of a dimensionless concentration variable, which is defined as the product of the protein concentration (c_2) and intrinsic viscosity, $[\eta]$. This successful reduction of viscosity for a range of $c_2 [\eta] \leq 0.1$ lends some support for the polymeric nature of antibodies in solution, as solutions of synthetic polymers show similar reduction. However,

while there is agreement of the trend in the reported k_H data with the magnitude of B_{22}, these measurements clearly indicate that these antibodies cannot be quantitatively modeled as either simple hard spheres or as flexible uncharged polymers. Instead, these measurements point to the existence of significant attractive interactions between the antibody molecules that cause the viscosity to increase more rapidly than in the case where the protein molecules interact with each other by short-range interactions only. We suggest that these interactions derive from solvation and counter-ion association of these charged polymers, and potentially due to dipole–dipole interactions, and that these interactions need to be studied in depth in order to understand the molecular origin of the values of k_H that are reported. Nonetheless, k_H provides a valuable measure of protein–protein interaction in relation to the increase of solution viscosity, and this quantity should be useful in the design of protein formulations that minimize the increase of viscosity for a given protein therapeutic concentration. Developing a better molecular understanding of the interactions underlying k_H will be helpful in designing stable antibody formulations for clinical trials of therapeutics and vaccines, whose viscosity is tractable for self-administration device design.

To paraphrase Einstein's general comment on the development of models: "Everything should be made as simple as possible, but no simpler" [116].

References

1. Roberts, C.J. Therapeutic protein aggregation: Mechanisms, design, and control. *Trends Biotechnol.* **2014**, *32*, 372–380. [CrossRef] [PubMed]
2. De Young, L.R.; Fink, A.L.; Dill, K.A. Aggregation of globular proteins. *Acc. Chem. Res.* **1993**, *26*, 614–620. [CrossRef]
3. Baek, Y.; Zydney, A.L. Intermolecular interactions in highly concentrated formulations of recombinant therapeutic proteins. *Curr. Opin. Biotechnol.* **2018**, *53*, 59–64. [CrossRef]
4. Amin, S.; Barnett, G.V.; Pathak, J.A.; Roberts, C.J.; Sarangapani, P.S. Protein aggregation, particle formation, characterization & rheology. *Curr. Opin. Colloid Interface Sci.* **2014**, *19*, 438–449.
5. Zhang, Z.; Liu, Y. Recent progresses of understanding the viscosity of concentrated protein solutions. *Curr. Opin. Chem. Eng.* **2017**, *16*, 48–55. [CrossRef]
6. Shire, S.J.; Shahrokh, Z.; Liu, J. Challenges in the development of high protein concentration formulations. *J. Pharm. Sci.* **2004**, *93*, 1390–1402. [CrossRef]
7. Wang, W. Protein aggregation and its inhibition in biopharmaceutics. *Int. J. Pharm.* **2005**, *289*, 1–30. [CrossRef]
8. Liu, J.; Nguyen, M.D.; Andya, J.D.; Shire, S.J. Reversible self-association increases the viscosity of a concentrated monoclonal antibody in aqueous solution. *J. Pharm. Sci.* **2005**, *94*, 1928–1940. [CrossRef] [PubMed]

9.   Jiskoot, W.; Randolph, T.W.; Volkin, D.B.; Middaugh, C.R.; Schöneich, C.; Winter, G.; Friess, W.; Crommelin, D.J.; Carpenter, J.F. Protein instability and immunogenicity: Roadblocks to clinical application of injectable protein delivery systems for sustained release. *J. Pharm. Sci.* **2012**, *101*, 946–954. [CrossRef]

10.   Carpenter, J.F.; Randolph, T.W.; Jiskoot, W.; Crommelin, D.J.; Middaugh, C.R.; Winter, G.; Fan, Y.X.; Kirshner, S.; Verthelyi, D.; Kozlowski, S. Overlooking subvisible particles in therapeutic protein products: Gaps that may compromise product quality. *J. Pharm. Sci.* **2009**, *98*, 1201–1205. [CrossRef]

11.   Rosenberg, A.S. Effects of protein aggregates: An immunologic perspective. *AAPS J.* **2006**, *8*, E501–E507. [CrossRef]

12.   Tanford, C. *Physical Chemistry of Macromolecules*; Wiley: Hoboken, NJ, USA, 1961.

13.   Yamakawa, H. *Modern Theory of Polymer Solutions*; Harper & Row: Manhattan, NY, USA, 1971.

14.   Sarangapani, P.S.; Hudson, S.D.; Jones, R.L.; Douglas, J.F.; Pathak, J.A. Critical examination of the colloidal particle model of globular proteins. *Biophys. J.* **2015**, *108*, 724–737. [CrossRef] [PubMed]

15.   Sarangapani, P.S.; Hudson, S.D.; Migler, K.B.; Pathak, J.A. The limitations of an exclusively colloidal view of protein solution hydrodynamics and rheology. *Biophys. J.* **2013**, *105*, 2418–2426. [CrossRef]

16.   Sarangapani, P.S.; Weaver, J.; Parupudi, A.; Besong, T.M.; Adams, G.G.; Harding, S.E.; Manikwar, P.; Castellanos, M.M.; Bishop, S.M.; Pathak, J.A. Both reversible self-association and structural changes underpin molecular viscoelasticity of mAb solutions. *J. Pharm. Sci.* **2016**, *105*, 3496–3506. [CrossRef]

17.   Liu, H.; Kumar, S.K.; Sciortino, F. Vapor-liquid coexistence of patchy models: Relevance to protein phase behavior. *J. Chem. Phys.* **2007**, *127*, 084902. [CrossRef]

18.   Dima, R.I.; Thirumalai, D. Asymmetry in the shapes of folded and denatured states of proteins. *J. Phys. Chem. B* **2004**, *108*, 6564–6570. [CrossRef]

19.   Kastelic, M.; Kalyuzhnyi, Y.V.; Hribar-Lee, B.; Dill, K.A.; Vlachy, V. Protein aggregation in salt solutions. *Proc. Natl. Acad. Sci.* **2015**, *112*, 6766–6770. [CrossRef] [PubMed]

20.   Russel, W.B. The Huggins coefficient as a means for characterizing suspended particles. *J. Chem. Soc. Faraday Trans. 2 Mol. Chem. Phys.* **1984**, *80*, 31–41. [CrossRef]

21.   Batchelor, G. Brownian diffusion of particles with hydrodynamic interaction. *J. Fluid Mech.* **1976**, *74*, 1–29. [CrossRef]

22.   Baxter, R. Percus–Yevick equation for hard spheres with surface adhesion. *J. Chem. Phys.* **1968**, *49*, 2770–2774. [CrossRef]

23.   Bicerano, J.; Douglas, J.F.; Brune, D.A. Model for the viscosity of particle dispersions. *J. Macromol. Sci. Rev. Macromol. Chem. Phys.* **1999**, *C39*, 561–642. [CrossRef]

24.   Kholodenko, A.L.; Douglas, J.F. Generalized Stokes-Einstein equation for spherical particle suspensions. *Phys. Rev. E* **1995**, *51*, 1081. [CrossRef]

25.   Douglas, J.F.; Freed, K.F. Competition between Hydrodynamic Screening ("Draining") and Excluded Volume Interactions in an Isolated Polymer Chain. *Macromolecules* **1994**, *27*, 6088–6099. [CrossRef]

26.   Kingsbury, J.S.; Saini, A.; Auclair, S.M.; Fu, L.; Lantz, M.M.; Halloran, K.T.; Calero-Rubio, C.; Schwenger, W.; Airiau, C.Y.; Zhang, J. A single molecular descriptor to predict solution behavior of therapeutic antibodies. *Sci. Adv.* **2020**, *6*, eabb0372. [CrossRef]

27.   Douglas, J.F.; Curtis, R.; Sarangapani, P.S.; Hudson, S.D.; Jones, R.L.; Pathak, J.A. Hard Spheres with Purely Repulsive Interactions Have Positive Diffusion Interaction Parameter, k_D. *Biophys. J.* **2017**, *113*, 753–754. [CrossRef]

28.   Batchelor, G. The effect of Brownian motion on the bulk stress in a suspension of spherical particles. *J. Fluid Mech.* **1977**, *83*, 97–117. [CrossRef]

29.   Yadav, S.; Liu, J.; Shire, S.J.; Kalonia, D.S. Specific interactions in high concentration antibody solutions resulting in high viscosity. *J. Pharm. Sci.* **2010**, *99*, 1152–1168. [CrossRef]

30.   Lilyestrom, W.G.; Yadav, S.; Shire, S.J.; Scherer, T.M. Monoclonal antibody self-association, cluster formation, and rheology at high concentrations. *J. Phys. Chem. B* **2013**, *117*, 6373–6384. [CrossRef]

31.   Fukuda, M.; Moriyama, C.; Yamazaki, T.; Imaeda, Y.; Koga, A. Quantitative correlation between viscosity of concentrated MAb solutions and particle size parameters obtained from small-angle X-ray scattering. *Pharm. Res.* **2015**, *32*, 3803–3812. [CrossRef] [PubMed]

32.   Godfrin, P.D.; Zarraga, I.E.; Zarzar, J.; Porcar, L.; Falus, P.; Wagner, N.J.; Liu, Y. Effect of hierarchical cluster formation on the viscosity of concentrated monoclonal antibody formulations studied by neutron scattering. *J. Phys. Chem. B* **2016**, *120*, 278–291. [CrossRef] [PubMed]

33.   Chiti, F.; Webster, P.; Taddei, N.; Clark, A.; Stefani, M.; Ramponi, G.; Dobson, C.M. Designing conditions for in vitro formation of amyloid protofilaments and fibrils. *Proc. Natl. Acad. Sci. USA* **1999**, *96*, 3590–3594. [CrossRef] [PubMed]

34.   Chari, R.; Jerath, K.; Badkar, A.V.; Kalonia, D.S. Long-and short-range electrostatic interactions affect the rheology of highly concentrated antibody solutions. *Pharm. Res.* **2009**, *26*, 2607. [CrossRef]

35.   Guijarro, J.I.; Sunde, M.; Jones, J.A.; Campbell, I.D.; Dobson, C.M. Amyloid fibril formation by an SH3 domain. *Proc. Natl. Acad. Sci. USA* **1998**, *95*, 4224–4228. [CrossRef] [PubMed]

36.   Ramírez-Alvarado, M.; Merkel, J.S.; Regan, L. A systematic exploration of the influence of the protein stability on amyloid fibril formation in vitro. *Proc. Natl. Acad. Sci. USA* **2000**, *97*, 8979–8984. [CrossRef]

37.   Fezoui, Y.; Hartley, D.M.; Walsh, D.M.; Selkoe, D.J.; Osterhout, J.J.; Teplow, D.B. A de novo designed helix-turn-helix peptide forms nontoxic amyloid fibrils. *Nat. Struct. Biol.* **2000**, *7*, 1095–1099. [CrossRef]

38.   Fändrich, M.; Fletcher, M.A.; Dobson, C.M. Amyloid fibrils from muscle myoglobin. *Nature* **2001**, *410*, 165–166. [CrossRef]

39. Kastritis, P.L.; Bonvin, A.M. On the binding affinity of macromolecular interactions: Daring to ask why proteins interact. *J. R. Soc. Interface* **2013**, *10*, 20120835. [CrossRef]
40. Thirumalai, D.; Klimov, D.; Dima, R. Emerging ideas on the molecular basis of protein and peptide aggregation. *Curr. Opin. Struct. Biol.* **2003**, *13*, 146–159. [CrossRef]
41. Tomar, D.S.; Li, L.; Broulidakis, M.P.; Luksha, N.G.; Burns, C.T.; Singh, S.K.; Kumar, S. In-silico prediction of concentration-dependent viscosity curves for monoclonal antibody solutions. In *mAbs*; Taylor & Francis: Abingdon, UK, 2017; pp. 476–489.
42. Trier, N.; Hansen, P.; Houen, G. Peptides, antibodies, peptide antibodies and more. *Int. J. Mol. Sci.* **2019**, *20*, 6289. [CrossRef]
43. Felder, C.E.; Prilusky, J.; Silman, I.; Sussman, J.L. A server and database for dipole moments of proteins. *Nucleic Acids Res.* **2007**, *35*, W512–W521. [CrossRef]
44. Takashima, S.; Asami, K. Calculation and measurement of the dipole moment of small proteins: Use of protein data base. *Biopolym. Orig. Res. Biomol.* **1993**, *33*, 59–68. [CrossRef]
45. Takashima, S. Electric dipole moments of globular proteins: Measurement and calculation with NMR and X-ray databases. *J. Non-Cryst. Solids* **2002**, *305*, 303–310. [CrossRef]
46. Antosiewicz, J.; Porschke, D. The nature of protein dipole moments: Experimental and calculated permanent dipole of .alpha.-chymotrypsin. *Biochemistry* **1989**, *28*, 10072–10078. [CrossRef]
47. Van Workum, K.; Douglas, J.F. Equilibrium polymerization in the Stockmayer fluid as a model of supermolecular self-organization. *Phys. Rev. E* **2005**, *71*, 031502. [CrossRef]
48. Van Workum, K.; Douglas, J.F. Symmetry, equivalence, and molecular self-assembly. *Phys. Rev. E* **2006**, *73*, 031502. [CrossRef] [PubMed]
49. Dudowicz, J.; Freed, K.F.; Douglas, J.F. Flory-Huggins model of equilibrium polymerization and phase separation in the Stockmayer fluid. *Phys. Rev. Lett.* **2004**, *92*, 045502. [CrossRef] [PubMed]
50. Brant, D.A.; Flory, P. The role of dipole interactions in determining polypeptide configurations. *J. Am. Chem. Soc.* **1965**, *87*, 663–664. [CrossRef]
51. Sali, D.; Bycroft, M.; Fersht, A.R. Stabilization of protein structure by interaction of alpha-helix dipole with a charged side chain. *Nature* **1988**, *335*, 740–743. [CrossRef] [PubMed]
52. Aqvist, J.; Luecke, H.; Quiocho, F.A.; Warshel, A. Dipoles localized at helix termini of proteins stabilize charges. *Proc. Natl. Acad. Sci. USA* **1991**, *88*, 2026–2030. [CrossRef]
53. Kirkwood, J.G.; Shumaker, J.B. Forces between protein molecules in solution arising from fluctuations in proton charge and configuration. *Proc. Natl. Acad. Sci. USA* **1952**, *38*, 863. [CrossRef]
54. Kirkwood, J.G.; Shumaker, J.B. The influence of dipole moment fluctuations on the dielectric increment of proteins in solution. *Proc. Natl. Acad. Sci. USA* **1952**, *38*, 855. [CrossRef]
55. Adžić, N.; Podgornik, R. Charge regulation in ionic solutions: Thermal fluctuations and Kirkwood-Schumaker interactions. *Phys. Rev. E* **2015**, *91*, 022715. [CrossRef]
56. Singh, S.N.; Yadav, S.; Shire, S.J.; Kalonia, D.S. Dipole-dipole interaction in antibody solutions: Correlation with viscosity behavior at high concentration. *Pharm. Res.* **2014**, *31*, 2549–2558. [CrossRef]
57. Ferreira, G.M.; Calero-Rubio, C.; Sathish, H.A.; Remmele, R.L., Jr.; Roberts, C.J. Electrostatically mediated protein-protein interactions for monoclonal antibodies: A combined experimental and coarse-grained molecular modeling approach. *J. Pharm. Sci.* **2019**, *108*, 120–132. [CrossRef]
58. Collins, K.D. The behavior of ions in water is controlled by their water affinity. *Q. Rev. Biophys.* **2019**, *52*, e11. [CrossRef] [PubMed]
59. Tomski, S.J.; Murphy, R.M. Kinetics of aggregation of synthetic β-amyloid peptide. *Arch. Biochem. Biophys.* **1992**, *294*, 630–638. [CrossRef]
60. Lomakin, A.; Chung, D.S.; Benedek, G.B.; Kirschner, D.A.; Teplow, D.B. On the nucleation and growth of amyloid beta-protein fibrils: Detection of nuclei and quantitation of rate constants. *Proc. Natl. Acad. Sci. USA* **1996**, *93*, 1125–1129. [CrossRef] [PubMed]
61. Yong, W.; Lomakin, A.; Kirkitadze, M.D.; Teplow, D.B.; Chen, S.-H.; Benedek, G.B. Structure determination of micelle-like intermediates in amyloid β-protein fibril assembly by using small angle neutron scattering. *Proc. Natl. Acad. Sci. USA* **2002**, *99*, 150–154. [CrossRef] [PubMed]
62. Xue, W.-F.; Homans, S.W.; Radford, S.E. Systematic analysis of nucleation-dependent polymerization reveals new insights into the mechanism of amyloid self-assembly. *Proc. Natl. Acad. Sci. USA* **2008**, *105*, 8926–8931. [CrossRef]
63. Niranjan, P.S.; Forbes, J.G.; Greer, S.C.; Dudowicz, J.; Freed, K.F.; Douglas, J.F. Thermodynamic regulation of actin polymerization. *J. Chem. Phys.* **2001**, *114*, 10573–10576. [CrossRef]
64. Niranjan, P.S.; Yim, P.B.; Forbes, J.G.; Greer, S.C.; Dudowicz, J.; Freed, K.F.; Douglas, J.F. The polymerization of actin: Thermodynamics near the polymerization line. *J. Chem. Phys.* **2003**, *119*, 4070–4084. [CrossRef]
65. Greer, S.C. Physical chemistry of equilibrium polymerization. *ACS Publ.* **1998**, *102*, 5413–5422. [CrossRef]
66. Sakamoto, A.; Ogata, D.; Shikata, T.; Urakawa, O.; Hanabusa, K. Large macro-dipoles generated in a supramolecular polymer of *N*, *N'*, *N''*-tris (3,7-dimethyloctyl) benzene-1,3,5-tricarboxamide in *n*-decane. *Polymer* **2006**, *47*, 956–960. [CrossRef]
67. Sear, R.P. Phase behavior of a simple model of globular proteins. *J. Chem. Phys.* **1999**, *111*, 4800–4806. [CrossRef]
68. Lomakin, A.; Asherie, N.; Benedek, G.B. Aeolotopic interactions of globular proteins. *Proc. Natl. Acad. Sci. USA* **1999**, *96*, 9465–9468. [CrossRef] [PubMed]

69. Cheung, J.K.; Shen, V.K.; Errington, J.R.; Truskett, T.M. Coarse-grained strategy for modeling protein stability in concentrated solutions. III: Directional protein interactions. *Biophys. J.* **2007**, *92*, 4316–4324. [CrossRef]

70. Gögelein, C.; Nägele, G.; Tuinier, R.; Gibaud, T.; Stradner, A.; Schurtenberger, P. A simple patchy colloid model for the phase behavior of lysozyme dispersions. *J. Chem. Phys.* **2008**, *129*, 08B615. [CrossRef] [PubMed]

71. Kastelic, M.; Dill, K.A.; Kalyuzhnyi, Y.V.; Vlachy, V. Controlling the viscosities of antibody solutions through control of their binding sites. *J. Mol. Liq.* **2018**, *270*, 234–242. [CrossRef] [PubMed]

72. Skar-Gislinge, N.; Ronti, M.; Garting, T.; Rischel, C.; Schurtenberger, P.; Zaccarelli, E.; Stradner, A. A colloid approach to self-assembling antibodies. *Mol. Pharm.* **2019**, *16*, 2394–2404. [CrossRef]

73. Esfandiary, R.; Parupudi, A.; Casas-Finet, J.; Gadre, D.; Sathish, H. Mechanism of reversible self-association of a monoclonal antibody: Role of electrostatic and hydrophobic interactions. *J. Pharm. Sci.* **2015**, *104*, 577–586. [CrossRef]

74. Majumdar, R.; Manikwar, P.; Hickey, J.M.; Samra, H.S.; Sathish, H.A.; Bishop, S.M.; Middaugh, C.R.; Volkin, D.B.; Weis, D.D. Effects of salts from the Hofmeister series on the conformational stability, aggregation propensity, and local flexibility of an IgG1 monoclonal antibody. *Biochemistry* **2013**, *52*, 3376–3389. [CrossRef] [PubMed]

75. Roberts, D.; Keeling, R.; Tracka, M.; Van Der Walle, C.; Uddin, S.; Warwicker, J.; Curtis, R. The role of electrostatics in protein–protein interactions of a monoclonal antibody. *Mol. Pharm.* **2014**, *11*, 2475–2489. [CrossRef] [PubMed]

76. Teilum, K.; Olsen, J.G.; Kragelund, B.B. Functional aspects of protein flexibility. *Cell Mol. Life Sci.* **2009**, *66*, 2231–2247. [CrossRef]

77. Kamerzell, T.J.; Middaugh, C.R. The complex inter-relationships between protein flexibility and stability. *J. Pharm. Sci.* **2008**, *97*, 3494–3517. [CrossRef]

78. Vargas-Lara, F.; Starr, F.W.; Douglas, J.F. Molecular rigidity and enthalpy–entropy compensation in DNA melting. *Soft Matter* **2017**, *13*, 8309–8330. [CrossRef] [PubMed]

79. Grünberg, R.; Nilges, M.; Leckner, J. Flexibility and conformational entropy in protein-protein binding. *Structure* **2006**, *14*, 683–693. [CrossRef]

80. Zimmermann, J.; Oakman, E.L.; Thorpe, I.F.; Shi, X.; Abbyad, P.; Brooks, C.L.; Boxer, S.G.; Romesberg, F.E. Antibody evolution constrains conformational heterogeneity by tailoring protein dynamics. *Proc. Natl. Acad. Sci. USA* **2006**, *103*, 13722–13727. [CrossRef] [PubMed]

81. Thorpe, I.F.; Brooks, C.L. Molecular evolution of affinity and flexibility in the immune system. *Proc. Natl. Acad. Sci. USA* **2007**, *104*, 8821–8826. [CrossRef]

82. Jimenez, R.; Salazar, G.; Yin, J.; Joo, T.; Romesberg, F.E. Protein dynamics and the immunological evolution of molecular recognition. *Proc. Natl. Acad. Sci. USA* **2004**, *101*, 3803–3808. [CrossRef]

83. Teague, S.J. Implications of protein flexibility for drug discovery. *Nat. Rev. Drug Discov.* **2003**, *2*, 527–541. [CrossRef]

84. Shoichet, B.K. Virtual screening of chemical libraries. *Nature* **2004**, *432*, 862–865. [CrossRef] [PubMed]

85. Schneider, G. Virtual screening: An endless staircase? *Nat. Rev. Drug Discov.* **2010**, *9*, 273–276. [CrossRef]

86. Zhou, T.; Georgiev, I.; Wu, X.; Yang, Z.-Y.; Dai, K.; Finzi, A.; Do Kwon, Y.; Scheid, J.F.; Shi, W.; Xu, L. Structural basis for broad and potent neutralization of HIV-1 by antibody VRC01. *Science* **2010**, *329*, 811–817. [CrossRef]

87. Rudicell, R.S.; Do Kwon, Y.; Ko, S.-Y.; Pegu, A.; Louder, M.K.; Georgiev, I.S.; Wu, X.; Zhu, J.; Boyington, J.C.; Chen, X. Enhanced potency of a broadly neutralizing HIV-1 antibody in vitro improves protection against lentiviral infection in vivo. *J. Virol.* **2014**, *88*, 12669–12682. [CrossRef]

88. Huang, J.; Kang, B.H.; Ishida, E.; Zhou, T.; Griesman, T.; Sheng, Z.; Wu, F.; Doria-Rose, N.A.; Zhang, B.; McKee, K. Identification of a CD4-binding-site antibody to HIV that evolved near-pan neutralization breadth. *Immunity* **2016**, *45*, 1108–1121. [CrossRef] [PubMed]

89. Rubinstein, M.; Colby, R.H. *Polymer Physics*; Oxford University Press: Oxford, UK, 2003; Volume 23.

90. Calero-Rubio, C.; Saluja, A.; Sahin, E.; Roberts, C.J. Predicting High-Concentration Interactions of Monoclonal Antibody Solutions: Comparison of Theoretical Approaches for Strongly Attractive Versus Repulsive Conditions. *J. Phys. Chem. B* **2019**, *123*, 5709–5720. [CrossRef]

91. Calero-Rubio, C.; Saluja, A.; Roberts, C.J. Coarse-Grained Antibody Models for "Weak" Protein–Protein Interactions from Low to High Concentrations. *J. Phys. Chem. B* **2016**, *120*, 6592–6605. [CrossRef] [PubMed]

92. Calero-Rubio, C.; Strab, C.M.; Barnett, G.V.; Roberts, C.J. Protein Partial Molar Volumes in Multi-Component Solutions from the Perspective of Inverse Kirkwood-Buff Theory. *J. Phys. Chem. B* **2017**, *121*, 5897–5907. [CrossRef]

93. Castellanos, M.M.; Pathak, J.A.; Colby, R.H. Both protein adsorption and aggregation contribute to shear yielding and viscosity increase in protein solutions. *Soft Matter* **2014**, *10*, 122–131. [CrossRef]

94. Barnett, G.V.; Qi, W.; Amin, S.; Lewis, E.N.; Roberts, C.J. Aggregate structure, morphology and the effect of aggregation mechanisms on viscosity at elevated protein concentrations. *Biophys. Chem.* **2015**, *207*, 21–29. [CrossRef]

95. Graessley, W.W. *Polymeric Liquids and Networks: Dynamics and Rheology*; Garland Science: New York, NY, USA, 2008.

96. Matsuoka, S.; Cowman, M. Equation of state for polymer solution. *Polymer* **2002**, *43*, 3447–3453. [CrossRef]

97. Yadav, S.; Shire, S.J.; Kalonia, D.S. Factors affecting the viscosity in high concentration solutions of different monoclonal antibodies. *J. Pharm. Sci.* **2010**, *99*, 4812–4829. [CrossRef]

98. Pamies, R.; Cifre, J.G.H.; Martínez, M.d.C.L.; de la Torre, J.G. Determination of intrinsic viscosities of macromolecules and nanoparticles. *Comparison of single-point and dilution procedures. Colloid Polym. Sci.* **2008**, *286*, 1223–1231.

99. Berry, G.C. Thermodynamic and conformational properties of polystyrene. II. Intrinsic viscosity studies on dilute solutions of linear polystyrenes. *J. Chem. Phys.* **1967**, *46*, 1338–1352. [CrossRef]

100. Grünberger, A.; Lai, P.-K.; Blanco, M.A.; Roberts, C.J. Coarse-Grained Modeling of Protein Second Osmotic Virial Coefficients: Sterics and Short-Ranged Attractions. *J. Phys. Chem. B* **2013**, *117*, 763–770. [CrossRef]

101. Calero-Rubio, C.; Ghosh, R.; Saluja, A.; Roberts, C.J. Predicting Protein-Protein Interactions of Concentrated Antibody Solutions Using Dilute Solution Data and Coarse-Grained Molecular Models. *J. Pharm. Sci.* **2018**, *107*, 1269–1281. [CrossRef] [PubMed]

102. Prausnitz, J. The fallacy of misplaced concreteness. *Biophys. J.* **2015**, *108*, 453. [CrossRef]

103. De Gennes, P.-G.; Gennes, P.-G. *Scaling Concepts in Polymer Physics*; Cornell University Press: Ithaca, NY, USA, 1979.

104. Freed, K.F. *Renormalization Group Theory of Macromolecules*; J. Wiley: Hoboken, NJ, USA, 1987.

105. McQuarrie, D.A. *Statistical Thermodynamics*; Harper & Row: New York, NY, USA, 1973.

106. Batchelor, C.K.; Batchelor, G. *An Introduction to Fluid Dynamics*; Cambridge University Press: Cambridge, UK, 1967.

107. Guazzelli, E.; Morris, J.F. *A Physical Introduction to Suspension Dynamics*; Cambridge University Press: Cambridge, UK, 2011; Volume 45.

108. Einstein, A. *Investigations on the Theory of the Brownian Movement*; Courier Corporation: Chelmsford, MA, USA, 1956.

109. Freed, K.F.; Edwards, S. Huggins coefficient for the viscosity of polymer solutions. *J. Chem. Phys.* **1975**, *62*, 4032–4035. [CrossRef]

110. Muthukumar, M.; Freed, K.F. Huggins coefficient for polymer solutions with excluded volume. *Macromolecules* **1977**, *10*, 899–906. [CrossRef]

111. Yamakawa, H. Concentration dependence of polymer chain configurations in solution. *J. Chem. Phys.* **1961**, *34*, 1360–1372. [CrossRef]

112. Sønderby, P.; Bukrinski, J.T.; Hebditch, M.; Peters, G.H.J.; Curtis, R.A.; Harris, P. Self-Interaction of Human Serum Albumin: A Formulation Perspective. *ACS Omega* **2018**, *3*, 16105–16117. [CrossRef] [PubMed]

113. McBride, C.; Lomba, E. Hard biaxial ellipsoids revisited: Numerical results. *Fluid Phase Equilibria* **2007**, *255*, 37–45. [CrossRef]

114. Yadav, S.; Laue, T.M.; Kalonia, D.S.; Singh, S.N.; Shire, S.J. The influence of charge distribution on self-association and viscosity behavior of monoclonal antibody solutions. *Mol. Pharm.* **2012**, *9*, 791–802. [CrossRef] [PubMed]

115. Van Rijssel, J.; Peters, V.; Meeldijk, J.; Kortschot, R.; van Dijk-Moes, R.; Petukhov, A.V.; Erne, B.; Philipse, A. Size-dependent second virial coefficients of quantum dots from quantitative cryogenic electron microscopy. *J. Phys. Chem. B* **2014**, *118*, 11000–11005. [CrossRef]

116. Sessions, R. How a 'difficult' composer gets that way. *New York Times*, 8 January 1950; 89.